



Universidad  
Carlos III de Madrid



This is a postprint version of the following published document:

N. Encinas, R.G. Dillingham, B.R. Oakley, J. Abenojar, M.A. Martínez, and M. Pantoja. *Atmospheric pressure plasma hydrophilic modification of a silicone surface*, Presented in part at the 1st International Conference on Structural Adhesive Bonding (AB2011), Porto, Portugal, 7–8 July 2011. *The Journal of Adhesion*, 88:4-6 (2012), pp. 321-336

DOI: [10.1080/00218464.2012.659994](https://doi.org/10.1080/00218464.2012.659994)

© Taylor & Francis Group, LLC (2012)

# Atmospheric Pressure Plasma Hydrophilic Modification of a Silicone Surface

N. ENCINAS<sup>1</sup>, R. G. DILLINGHAM<sup>2</sup>, B. R. OAKLEY<sup>2</sup>, J. ABENOJAR<sup>1</sup>,  
M. A. MARTÍNEZ<sup>1</sup>, and M. PANTOJA<sup>1</sup>

<sup>1</sup>Materials Science and Engineering Department, IAAB, Materials Performance Group,  
Universidad Carlos III de Madrid, Leganés, Madrid, Spain

<sup>2</sup>Brighton Technologies Group Inc., Cincinnati, Ohio, USA

*The aim of this study was the creation of a silicone hydrophilic surface prior to bonding. Modifications in wettability and adhesion properties of silicone were performed with an atmospheric plasma torch (APPT). Surface energy variations of the substrate, both pristine and APPT-treated, were evaluated through contact angle measurements, studying the hydrophobic recovery of the samples up to 24 hours of aging. Compositional and topographical changes induced by APPT and aging were studied by attenuated total multiple reflection mode infrared spectroscopy (ATR-FTIR), X-ray photoelectron spectroscopy (XPS), mechanical profilometry, scanning electron microscopy (SEM), and atomic force microscopy (AFM), respectively. Adhesion pull-off tests were performed on silicone-aluminium stud joints using three commercial adhesives, which were Sikaflex<sup>®</sup>-252, polyurethane-based, Loctite<sup>®</sup>-330, urethane methacrylate ester-based acrylic, and Terostat<sup>®</sup>-922, modified silicone. Although experimental data of all the bonding specimens led to an undesired adhesive failure, it was found that APPT-treated samples gave higher adhesive strength than the pristine ones, which was explained by the higher surface energy, thus more wettable material, after APPT. This effect remained stable for just 1 h, when the substrate began its hydrophobic recovery, reaching the original surface energy values after 24 h of aging.*

---

Presented in part at the 1st International Conference on Structural Adhesive Bonding (AB2011), Porto, Portugal, 7-8 July 2011.

Address correspondence to N. Encinas, Materials Science and Engineering Department, IAAB, Materials Performance Group, Universidad Carlos III de Madrid, Av. Universidad, 30, 28911 Leganés, Madrid, Spain. E mail: nencinas@ing.uc3m.es

*KEYWORDS Atmospheric pressure plasma; Hydrophobic recovery; Polymeric adhesion; Silicone*

## 1. INTRODUCTION

Silicone polymers correspond to the family of polydialkylsiloxanes, with the general formula  $-(\text{Si}(\text{R}_2)\text{-O})_n-$ , the most common of which are those terminated with trimethylsilyloxy groups, called polydimethylsiloxanes (PDMS) [1]. These elastomeric materials are often used in medical applications like ocular lenses, syringes, or implants, due to properties such as chemical inertness, low-cost, versatility, and high oxygen permeability [2]. This material finds other fields of application such as anti-fouling adhesion thanks to its soft surface, or insulation [3], where its hydrophobicity gives it the property of wetting resistance. But this naturally hydrophobic behaviour also appears to be the most important shortcoming of silicone. Its low surface energy and, thus, very poor adhesion properties, makes it necessary to functionalize and modify silicone prior to use. The increase in silicone surface energy can be accomplished by means of diverse methods, physical or chemical, which implies the introduction of polar moieties. One of the most popular methods for this aim is to add surfactants to the bulk material [4,5] and the use of chemical promoters such as organosilanes [6], but it implies the use of pollutant solvents, which are environmentally not friendly.

The use of plasma treatments to modify polymeric surfaces presents great advantages: treatment on the outermost surface layer without affecting bulk properties, versatility in the treatment of various materials, the involvement of fast and easy experiments with controllable parameters, the prevention of toxic waste use or generation, and the non-heating of the samples [7–9]. They primarily act on a surface by cleaning, etching, and introducing new functionalities, by two possible mechanisms: (a) surface grafting or (b) breakdown of polymer chains and reaction of radical fragments with active species. A crosslinking reaction may also take place in the inner surface layers.

Many authors have previously presented important works on PDMS surface modification by oxygen plasma treatments [10–12]. They found evidences of a deep propagation of oxygen plasma effects to a hundred nanometers, and a hydrophobic recovery after aging assumed to be caused by the migration of low molecular weight (LMW) oxygen-containing species from the surface to the bulk of the material. A deeper study of hydrophobic recovery of silicone rubbers was carried out by Hillborg and Gedde [13], suggesting the following mechanisms:

- (i) Migration of LMW species from bulk to surface;
- (ii) Reorientation of polar groups existing at the surface to the bulk polymer;
- (iii) Condensation of Si-OH groups at the polymer surface;

- (iv) Surface adsorption of environmental contamination;
- (v) Loss of oxygen containing functionalities by volatilization;
- (vi) Variations of the sample roughness.

The present work deals with the observation of the surface modifications and evolution with aging of silicone samples exposed to APPT. Some of the main differences between APPT and vacuum processes are the existence of higher temperature ionic species and lack of vacuum ultraviolet (VUV) light. These differences have the potential to alter the surface *via* diverse reaction mechanisms and result in various functional groups, or at least a different balance of exposed moieties.

The use of APPT devices is an interesting way to treat polymers, as it has the possibility of performing in-line experiments and allows fast and low-cost processes due to the elimination of a vacuum step [8, 14]. This work was focused on the surface modification of a commercial silicone material, available to be industrially used. The selected APPT technique allowed the creation of a experimental procedure that could be used in a continuous process. The hydrophobic recovery study of the silicone surface after treatment was carried out by means of contact angle measurements and surface energy calculations, attenuated total multiple reflection mode infrared spectroscopy (ATR-FTIR), X-ray photoelectron spectroscopy (XPS), mechanical profilometry, scanning electron microscopy (SEM), and atomic force microscopy (AFM). Mechanical pull-off tests of the adhesive bonding of the silicone, both as-received and APPT-treated, bonded with modified silicone rubber, one-component polyurethane, and acrylic adhesives were performed, comparing the results of the samples APPT-treated and untreated.

## 2. EXPERIMENTAL

### 2.1. Materials

Commercial PDMS samples (Ketersa, Madrid, Spain) were used. Before every contact angle measurement or APPT treatment, specimens were softly wiped (in order to avoid the scratching of the samples) with methylethylketone (MEK), allowing evaporation of the solvent. Further characterization of the as-received samples revealed the existence of a remaining talc film ( $Mg_3Si_4O_{10}(OH)_2$ ) on the PDMS surface, due to the manufacturing process. For the adhesion study, three types of adhesives were chosen, which were Sikaflex<sup>®</sup>-252 polyurethane one-component-based structural adhesive (PU; Sika Corporation, Madison Heights, MI, USA), Loctite<sup>®</sup>-330 urethane methacrylate ester-based acrylic adhesive (AC Loctite, Dublin, Ireland), and Terostat<sup>®</sup>-922-modified silicone adhesive (MS; Henkel, Düsseldorf, Germany). The AC adhesive needed to be used in combination with a Loctite-737 activator

(Loctite, Dublin, Ireland), applied on the metallic part of the system. The mechanical properties of the adhesives are described in Table 1.

## 2.2. Surface Modification

Plasma treatment was achieved by using a Plasmacreat GmbH (Steinhagen, Germany) APPT device, the operating characteristics of which are described in Table 2. The system is equipped with a mobile platform in which the sample is placed, as it is described elsewhere [15].

After APPT treatment, silicone samples were subjected to 15 min, 45 min, 1 h, 2 h, 3 h, 4 h, 6 h, and 24 h of aging under room temperature (24°C) and 35% relative humidity.

## 2.3. Attenuated Total Multiple Reflection Spectroscopy

A Bruker Tensor™ 27 (Bruker Optik GmbH, Madrid, Spain) spectrometer was used to obtain the infrared spectra of untreated and treated samples, both freshly treated and aged. A diamond prism was used with an incident angle of the IR radiation of 45° and 32 scans with a resolution of 4 cm<sup>-1</sup>. Spectra were recorded from 600 to 4000 cm<sup>-1</sup>, giving information on the chemical compositions of the materials at about 5–10 μm depth.

## 2.4. X-ray Photoelectron Spectroscopy

Chemical modifications on the outermost surface layer (about 5 nm) of the PDMS samples were analyzed with a Surface Science SSX-100 XPS spectrometer (Surface Science Western, Ontario, Canada) using a monochromated Al-K<sub>α</sub> X-ray source operating at 1486.6 eV and 200 W. All binding energies were referred to the C 1s core level spectrum position for C-C and C-H (hydrocarbons) species at 284.6 eV, subtracting a Shirley background. Variations in the silicon, carbon, and oxygen atomic content of PDMS surface after APPT were estimated, determining the level of oxidation achieved by the treatment.

## 2.5. Scanning Electron Microscopy (SEM)

A Philips, XL-30 FEI EUROPE SEM microscope (Eindhoven, Holland) with an electron beam energy of 20 kV was used to provide the analysis of the

**TABLE 1** Technical Data of the Adhesives

Adhesive	Curing mechanism	Shore A hardness	Shrinkage	Tensile strength (MPa)
Sikaflex 252	Moisture	55	6%	4.14
Terostat 922	With activator			12.22
Loctite 330	Moisture	55/60	<2%	3.3

**TABLE 2** Operating Parameters of the APPT Device

Gas	Air
Output pressure (bar)	2
Discharge tension (kV)	20
Frequency (kHz)	17
Rotation torch (rpm)	1900
$d_{\text{torch-sample}}$ (mm)	6
Speed (m/s)	0.2

physical modification of silicone with APPT and aging. Specimens were gold coated in a Polaron<sup>TM</sup> high resolution sputter coater prior to obtaining the SEM micrographs.

## 2.6. Atomic Force Microscopy and Roughness Measurements

The AFM studies were performed using a MultiMode Nanoscope<sup>®</sup> IV (Digital Instruments/Veeco Metrology Group, Santa Barbara, CA, USA). The AFM measurements were carried out at room temperature, operating in the tapping mode, employing silicon tips with a force constant of about 40 N/m and a resonance frequency close to 300 kHz, recording simultaneously height and phase images.

Direct measurements of the silicone roughness profiles both as-received and APPT-treated were also achieved using a Hommel Tester T8000 profilometer, following the DIN 4768 standard, yielding results of the average arithmetic roughness ( $R_a$ ) and the averaged distance from top to bottom of the samples ( $R_z$ ).

## 2.7. Contact Angle Measurement and Surface Energy Calculation

Sessile drop method measurements were performed with an OCA 15 plus device from DataPhysics (Neurtek Instruments, Eibar, Guipúzcoa, Spain). Static drops of 2  $\mu$ L of deionized water, glycerol, diiodomethane, nitromethane, and 1,5-pentanediol (surface tension components of which previously tabulated by other authors, are given in Table 3) were deposited onto smooth and uniform silicone samples and measured after stabilization of the drop.

**TABLE 3** Surface Tension Components of the Test Liquids Used for the OWRK and Good Calculus Method for Surface Energy. Data are in [mJ/m<sup>2</sup>]

Liquid	$\gamma_r$	$\gamma_D$	$\gamma_P$	$\gamma_r$	$\gamma^{LW}$	$\gamma_i^+$	$\gamma_i^-$
Deionized water	72.1	19.9	52.2	72.8	21.8	25.5	25.5
Glycerol	62.7	21.2	41.5	64.0	34.0	3.9	57.4
1,5 pentanediol	43.3	27.6	15.7				
Diiodomethane	50.0	47.4	2.6	50.8	50.8	0.0	0.0
Nitromethane	36.8	20.3	16.5				

Surface energy of silicone was evaluated before and after APPT treatment. Measurements on the treated surfaces included an aging study through different times, from the freshly treated samples to the hydrophobic recovery of silicone, which was estimated at approximately 24 h of storage.

Calculation of surface energy was achieved using two mathematical methods which take into account various components related to the forces found in the solid-liquid-vapour system formed when the drop is put on the solid surface.

The Owens-Wendt-Rable-Kaelble (OWRK) method [Eq. 1] takes the total surface energy of a solid as the sum of a dispersion parameter (due to London-type forces) and a polar parameter (which arises by the action of hydrogen bonding and dipole-dipole interactions in the system) [16].

$$\frac{(1 + \cos \theta) \cdot \gamma_l}{2\sqrt{\gamma_l^D}} = \sqrt{\gamma_s^P} \cdot \sqrt{\frac{\gamma_l^P}{\gamma_l^D}} + \sqrt{\gamma_s^D} \quad (1)$$

In this expression,  $\gamma_l$  and  $\gamma_s$  represent the surface tension of liquid and the surface energy of solid, respectively. The dispersive and polar fractions are identified by the D and P superscripts. The contact angle of the drop on the solid surface is represented by  $\theta$ . This method is the selected to understand the mechanism of a surface hydrophobic recovery.

On the other hand, Van Oss *et al.* [17] considered the surface energy as the sum of acid-base and Lifshitz-van der Waals interactions [Eq. 2.]. The first term includes London dispersion, Debye induction, and Keesom dipole-dipole additive forces, while the acid-base term comprises an electron donor and an electron acceptor component.

$$\gamma_l(1 + \cos \theta) = 2\sqrt{\gamma_l^{LW} \cdot \gamma_s^{LW}} + 2\left[\sqrt{\gamma_l^+ \cdot \gamma_s} + \sqrt{\gamma_l \cdot \gamma_s^+}\right] \quad (2)$$

Lifshitz-van der Waals interactions are represented by  $\gamma^{LW}$ .  $\gamma^-$  and  $\gamma^+$  terms are the electron donor and electron acceptor of the acid-base component of the surface energy,  $\gamma_s^{AB}$ , which derives from [Eq. 3]

$$\gamma_s^{AB} = 2\sqrt{\gamma^- \cdot \gamma^+} \quad (3)$$

The Van Oss *et al.* calculation method [17] results are adequate to study the effects of a surface treatment on the adhesive properties of the tested material.

## 2.8. Adhesion Tests

An adhesion Tester KN-10 device (Neurtek Instruments, Eibar, Guipúzcoa, Spain) was used to evaluate the modifications in adhesion properties of silicone after APPT treatment, using aluminium studs of 20 mm diameter

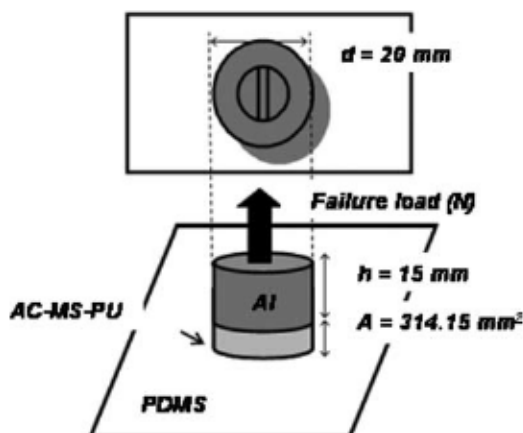


**FIGURE 1** Diagram of the adhesive bonding. An aluminium stud is set onto a PDMS sheet, using the three types of adhesives (AC, MS, and PU). Failure load of the samples is measured and transformed into tensile values by means of the adhesive bonding area (A).

and taking into account the necessary change in units from the failure load values (N) given by the machine to tension values (MPa). Ten samples per studied condition were tested. A diagram of the system used for the pull-off tests is shown in Fig. 1.

### 3. RESULTS AND DISCUSSION

#### 3.1. Chemical Modification Analysis by ATR-FTIR and XPS

The ATR-FTIR spectrum corresponding to the untreated and freshly treated PDMS samples is shown in Fig. 2. Comparing the peaks of the two samples, it is observed that APPT yields a modified polymeric surface characterized by the appearance of a low intensity absorption band at around  $3674\text{ cm}^{-1}$  (Fig. 2b, in detail). This peak is assumed to correspond to the hydroxyl of the isolated silanol groups (Si-OH) and not to water adsorption on the silicone surface. A decrease in intensity is also observed for the  $\text{CH}_3$  ( $1259$  and  $2954\text{ cm}^{-1}$ ) and  $\text{Si}-((\text{CH}_3)_2)$  ( $787\text{ cm}^{-1}$ ) bands, while the peaks which arise from Si-C ( $867\text{ cm}^{-1}$ ) and Si-O-Si ( $1008\text{ cm}^{-1}$ ) backbone components of silicone do not suffer any remarkable variation in intensity.

A strong shoulder near  $1100\text{ cm}^{-1}$  is observed in the spectrum of the untreated material (Fig. 2a). This peak reveals the existence of  $(\text{Mg}_3\text{Si}_4\text{O}_{10}(\text{OH})_2)$ , confirmed by the low intensity sharp band near  $3660\text{ cm}^{-1}$  (Fig. 2b, in detail). Bodas *et al.* studied the effects of oxygen plasma on addition-rubber silicone [18], demonstrating that the penetration depth of the treatment increased as the wave number decreased. They found that the oxygen surface modification went approximately 100 nm deep into the sample, as no changes



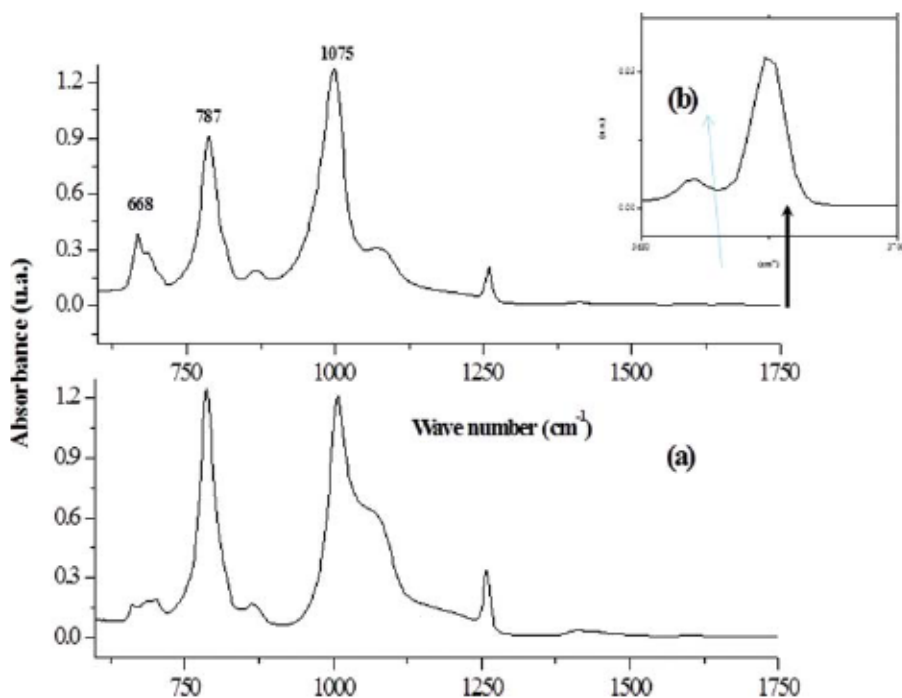


**FIGURE 2** ATR FTIR spectra of the silicone samples (a) as received and (b) APPT treated. In the detail is presented the new peak at  $3674\text{ cm}^{-1}$  which appears on the APPT PDMS. (Color figure available online.)

on the spectral intensity of surface bands, located at  $1015$  and  $785\text{ cm}^{-1}$ , was observed. In the present work, it is a decrease in  $\text{Si}((\text{CH}_3)_2)$  peak intensity of 27% that was found. This fact seems to confirm that a surface modification is taking place with the APPT treatment, eliminating methyl groups from the surface by linkage scission or reorienting them to the bulk. Zhu *et al.* explained the elimination of methyl groups on silicone surfaces subjected to corona discharge [19] by the fact that the energy of part of the plasma photons is larger than the binding energy of the  $\text{Si-O-Si}$  and  $\text{Si-CH}_3$  linkages. The reorientation of these groups to the bulk is explained on the basis of hydrophobic recovery, encouraging  $\text{Si-CH}_3$  to remain on the surface and for oxidized species to re-orient. In this case, it is assumed that APPT has high temperature ions and appreciable short wavelength light, so the loss of  $\text{Si-CH}_3$  could derive from ion impact.

Also, peaks corresponding to the PDMS surface layer, located at  $668$  and  $702\text{ cm}^{-1}$ , duplicate their intensity with treatment.

A deeper understanding of the outermost modifications is given by XPS analysis. Typically, APPT treatment of silicone removes  $\text{CH}_3$  and oxidizes the silicone to silica on the surface, but the data (Table 4) show a negligible oxidation of silicone when APPT is applied. The increase in carbon content

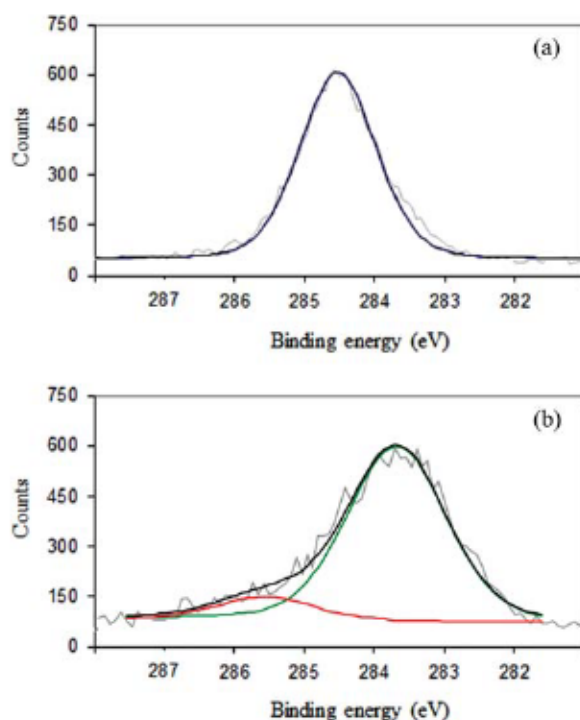
**TABLE 4** Elemental Composition of PDMS Both Pristine and APPT Treated

PDMS surface state	% C	% O	% Si
As received	43	31	26
APPT treated	47	32	18

and decrease in silicon seems to indicate that a reorientation of the surface functional groups is taking place, with silicon-containing moieties being buried into the bulk, while the carbon segments get more exposed.

Carbon 1s curve fitting of the as-received samples (Fig. 3a) shows a typical PDMS surface, adjusted to just one peak at a binding energy of 284.6 eV corresponding to the C-H linkages of the PDMS methyl groups. When the material is subjected to APPT (Fig. 3b), the C-O signal arises, confirming the insertion of oxidised polar functionalities in the PDMS surface.

The intensity of the C-O peak reveals that the extent of introduced polar groups in the PDMS surface is not as large as would be inferred from the FTIR-ATR spectra (Fig. 2), as Table 3 shows. These data suggest that it is possible that the effects of APPT on the silicone surface are taking place

**FIGURE 3** C 1s curve fitting of the PDMS (a) as received and (b) after APPT treatment. (Color figure available online.)

in a deeper layer of the material than that detected by XPS, *i.e.*, below the nanometer scale.

The analysis of the aging effects on the APPT-treated specimens assessed by ATR-FTIR is shown in Fig. 4. From these spectra it can be inferred that no differences are obtained for APPT silicone aged up to 24 h, resembling indeed the band intensities and the dramatic reduction of the peak area corresponding to the acid groups (shoulder at  $1074\text{ cm}^{-1}$ ). It has to be remarked that the spectrum of the untreated surface looks like it has a strong talc component while the spectra of the treated surfaces seem to be lacking in that.

These data suggest that a time stable APPT-treated silicone surface has been generated, which does not correlate with the hydrophobic recovery results after a short period of time obtained by other authors for plasma-treated PDMS [10].

### 3.2. Study of Hydrophobic Recovery through Surface Energy

In order to evaluate in depth the ATR-FTIR results, a surface energy study through aging time was achieved using contact angle measurements of deionized water, glycerol, diiodomethane, nitromethane, and 1,5-pentandiol.

It can be seen that APPT treatment increases, to an important extent, the PDMS surface energy (Fig. 5a), from an initial value of  $17.67 \pm 3.55\text{ mJ/m}^2$  for the pristine samples (due to the hydrophobic aliphatic groups surrounding

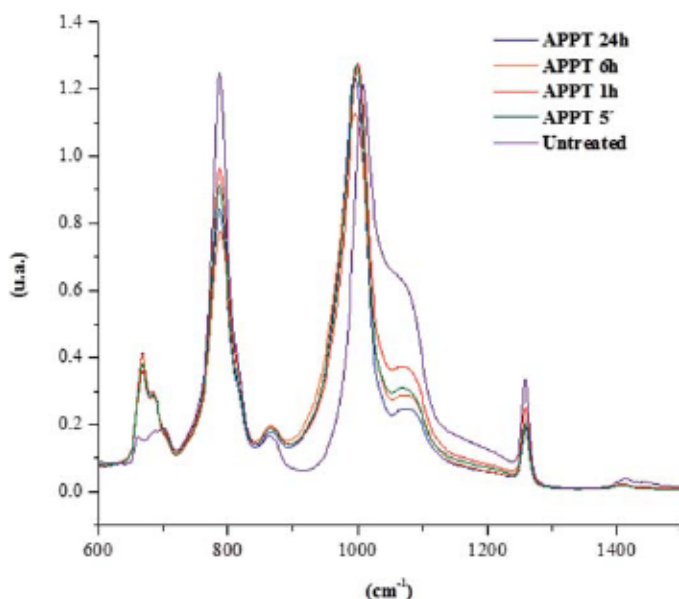


**FIGURE 4** ATR FTIR spectra of the pristine samples, APPT freshly treated, and aged up to 1, 6, and 24 h. (Color figure available online.)

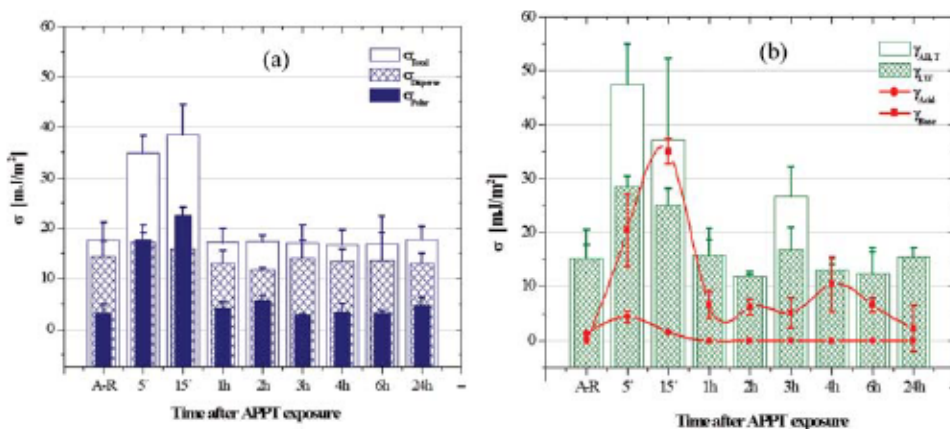


**FIGURE 5** Study of the PDMS surface energy subjected to APPT and aged for 24 h, calculated by the (a) OWRK method and (b) Van Oss and Good acid base approximation. (Color figure available online.)

the siloxane chains) to  $34.93.6 \pm 3.67 \text{ mJ/m}^2$  for the freshly treated ones. Surface energy suffers an almost linear increase during the first 15 minutes after APPT exposure and after that time begins to lower until a surface energy plateau is reached in 1 h, almost corresponding to the pristine data. It has to be remarked that this enhancement of surface energy is related to a higher polar fraction (82%), and presents the same behaviour as the total energy (a dramatic increase just after APPT exposure followed by a recovery until a plateau is achieved after 1 h), with a disperse component almost stable in all the conditions. This result is assumed to derive from the introduction of new functionalities of a polar nature, thus yielding hydrophilic behaviour. Considering the ATR-FTIR spectrum, changes in hydrophobicity are assumed to be caused by the appearance of the Si-OH moieties and the decrease on the amount of hydrophobic methyl groups from the PDMS surface. As was expected, the same tendency was observed for the results obtained by the acid-base approximation. The Lifshitz-Van der Waals component (Fig. 5b), which takes into account disperse interactions, suffers variations with APPT of 47%, which is reduced to 22% with aging. The most significant changes are observed for the Lewis base component, which is highly enhanced by APPT, from an almost null value to  $20.47 \pm 6.72 \text{ mJ/m}^2$ . Although this component begins to recover the initial value after aging 1 h, as was assumed considering the results of the components obtained by the OWRK method, the treated surface retained a certain electron-donor character. Variations in  $\gamma^{\text{AB}}$ ,  $\gamma^{\text{LW}}$ , and  $\gamma^-$  results are observed during aging, which is expected to be caused by the existence of heterogeneities in the PDMS samples, which affects the contact angle measurements due to the extreme dependence of this technique on the solid surface. The Lewis acid fraction was slightly increased with plasma and gradually recovers the native value.

### 3.3. Topographical Modifications of Silicone: SEM, AFM and Roughness Measurements

APPT treatment is known to produce not only chemical modifications on a polymer, but also surface etching [20]. The first attempt to evaluate variations in the silicone topography was achieved by obtaining the  $R_a$  and  $R_z$  roughness parameters using a mechanical profilometer (Fig. 6). Results show a slight roughness modification with APPT treatment, with a drop of  $R_a$  from 0.20 to 0.17  $\mu\text{m}$ , while the  $R_z$  parameter rises from 1.26 to 1.67  $\mu\text{m}$ , which is indicative of the generation of a most prominent peak-valley surface. The integration of the total surface roughness did not suffer significant variations.

A more exhaustive examination requires the acquisition of SEM images, shown in Fig. 7. The pristine surface (Fig. 7a) presents a smooth surface formed by homogeneously distributed cracks and some particle detachment. When PDMS is exposed to APPT (Fig. 7b), particles are removed from the surface or apparently coalesce, exhibiting higher micrometric averaged size. A similar surface was observed after 12 h of aging, so no physical recovery can be assumed from these results.

Another approach to the chemical composition of the studied samples was performed using the energy dispersive X-ray analysis (EDX) probe provided in the SEM device. As is shown in Table 5, PDMS specimens are mainly composed of a siloxane backbone (Si, O) with aliphatic functionalities (C). The existence of an amount of magnesium comparable to the carbon content is observed, which is assumed to come from the manufacture of the commercial material.

The surface of the samples in the native state, exposed to APPT and subjected to aging, was also examined using AFM microscopy (Fig. 8). It is

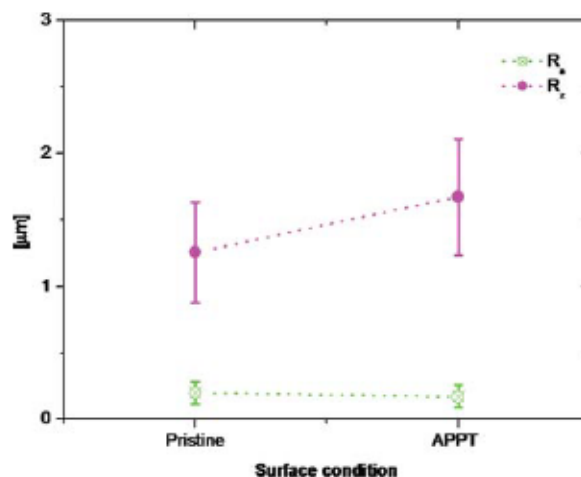


**FIGURE 6** Roughness parameters of the APPT treated and as received silicone. (Color figure available online.)

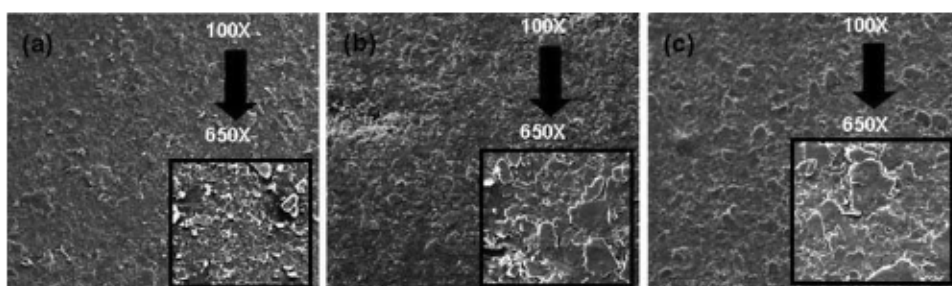


**FIGURE 7** 100× magnification SEM micrographs measured on the samples: (a) native, (b) immediately after APPT, and (c) aged 12 h. In detail are presented the 650× magnification images.

observed that the pristine surface (Fig. 8a), constituted of grooves and some dimpled zones distributed in a homogeneous way, suffers an important decrease in roughness with APPT, from 1.6 to 0.9  $\mu\text{m}$ , even though the difference between the top peak and the low valley is much more marked, as was expected from the profilometry results. After 15 min of aging, the surface peaks distribution begins to change, going through a maximum roughness of 2.1  $\mu\text{m}$  (Fig. 8c) to a 1.8  $\mu\text{m}$  plateau (Fig. 8d–e) achieved after aging 2 h. The final roughness after 24 h of storage differs only approximately 12% from the native one. These results confirm the data given by mechanical profilometry, which yielded a variation of 15% on the  $R_a$  roughness parameter between untreated and APPT-treated surfaces.

### 3.4. Adhesion Pull-Off Tests

The results of the adhesion tests are shown in Fig. 9. The first conclusion of the experiments is that the most suitable adhesive to bond this material with the aluminium studs is the AC, the tensile strength values of which are, for all the experimental conditions, approximately 25% and 60% higher than the MS and the PU results, respectively. The hydrophilic enhancement achieved by the exposure of PDMS substrates to APPT allows the attainment 37–23% better adhesion results. The most dramatic increase on adhesion with APPT is observed for the MS adhesive. The as-received surfaces yield 0.42 kPa, while the APPT samples are enhanced up to 0.67 kPa. The same recovery tendency

**TABLE 5** EDX Atomic Composition of the PDMS Surfaces Untreated, Freshly APPT treated, and 24 h Aged

Element	As received % At.	APPT % At.	APPT 24 h aged % At.
Si	30.92	31.21	30.43
O	34.96	35.56	33.62
C	21.82	22.01	22.96
Mg	12.30	11.42	12.99

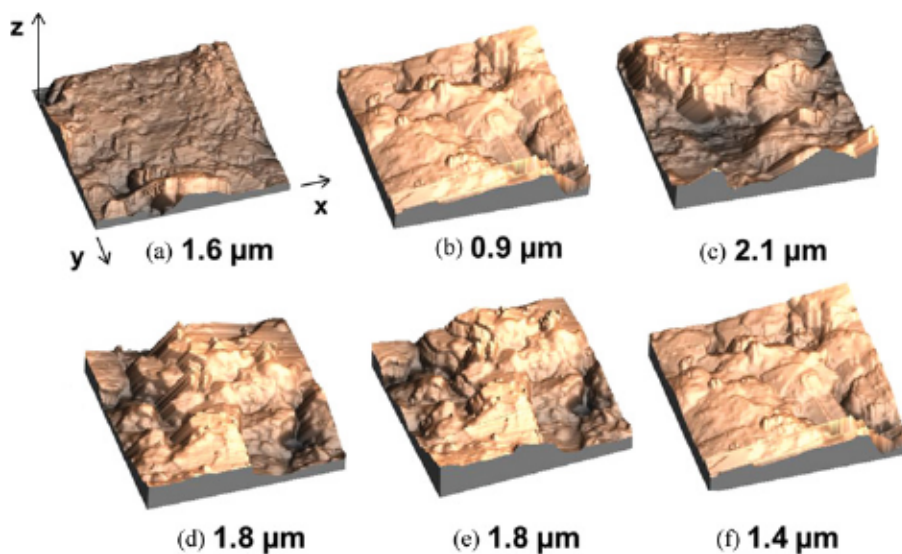


**FIGURE 8** ( $10 \times 10$ )  $\mu\text{m}^2$  area AFM images of (a) native silicone, (b) immediately APPT treated and aged (c) 15 min, (d) 2 h, (e) 3 h, and (f) 24 h. (Color figure available online.)

is found for the three adhesives, where the APPT tensile strength result tends to decrease with aging, at a rate of approximately 16% after the first hour, and 23% after a day.

Considering the surface energy and hydrophobic recovery mechanisms suggested by Hillborg and Gedde *et al.* [13], and taking into account the

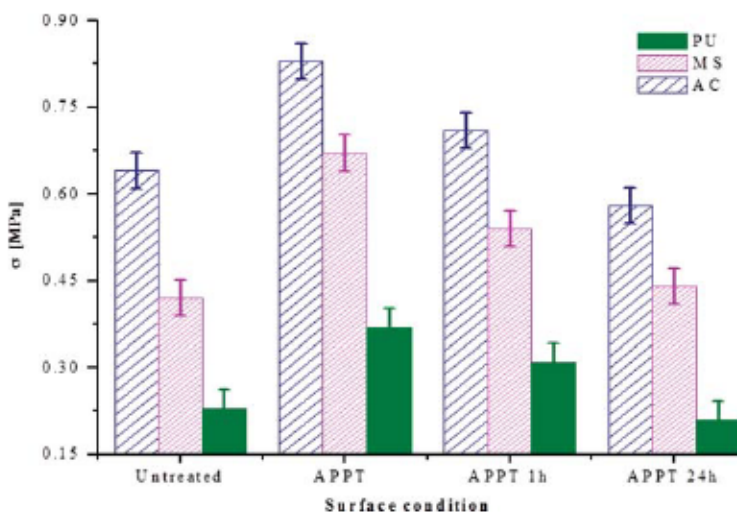


**FIGURE 9** Tensile strength results of the tested adhesive bonding. Experiments were performed on the untreated, freshly APPT treated, and aged for 1 and 24 h PDMS samples. (Color figure available online.)

experimental results obtained in this work, it can be assumed that the PDMS hydrophobic recovery is produced by a sum of effects, which are the possible migration of LMW fragments of the polymer from bulk to surface, the reorientation of hydrophilic surface groups to the bulk, induced changes in surface roughness during the aging process (although they considered this effect to be less likely to affect the recovery process, the experimental data indicate that a modification in roughness affects the adhesion properties), and, eventually, the consideration of adsorption of environmental pollutants.

No condensation of Si-OH groups at the surface can be assumed, because ATR-FTIR spectra present no significant differences between the APPT recently treated sample and the aged surfaces, showing the existence, in all of them, of the low intensity OH peak corresponding to silanol groups located at  $3674\text{ cm}^{-1}$ . It is also impossible to conclude that oxygen-containing functionalities have been lost, because both infrared, XPS, and EDX analysis show that the variations in the atomic weight oxygen percentage between untreated, APPT, and 24 h of aging samples are minimal.

#### 4. CONCLUSIONS

Commercial PDMS samples were exposed to APPT and subjected to aging in order to evaluate the possible modifications in surface energy, thus, adhesion properties, of the samples. It was observed that APPT indeed enhanced surface energy by achieving a more polar surface with a certain electron-donor character. Si-OH groups were introduced on to the polymeric surface, while hydrophobic methyl groups were removed or buried in the bulk of the polymer.

A decrease of the averaged total roughness was also observed for the freshly-treated samples, while the difference between the extreme peak-valley was enhanced.

A clear improvement in the PDMS adhesion properties was achieved, due both to the creation of a more hydrophilic surface susceptible to be wetted by the adhesive and the creation of a major anchoring area. Among the studied adhesives, AC presented the highest results for all the experimental conditions (0.58–0.83 kPa), while the low tensile strength values observed for the PU (0.23–0.37 kPa) made it the most unsuitable adhesive to be used in this system.

Hydrophobic recovery of the specimens took place in just 1 h of aging, yielding a reduction in surface energy (both total and polar), a recovery of roughness ( $1.4\text{ }\mu\text{m}$ ), and a decrease in adhesion.

Although all the samples yielded an adhesive failure mode, it was confirmed that APPT positively increases PDMS hydrophilic behaviour, and that this material tends to recover its native properties in a short period of time of just 1 h.



## ACKNOWLEDGMENTS

Financial support from the Universidad Carlos III de Madrid Foundation and Chemistry and Materials Technological Institute “Álvaro Alonso Barba” are acknowledged, as well as from the Universidad Pontificia Comillas (ICAI) (Spain).

## REFERENCES

- [1] De Buyl, F., *Int. J. Adhesion and Adhesives* **21**, 411–422 (2001).
- [2] Yager, P., Edwards, T., Fu, E., Helton, K., Nelson, K., and Tam, M. R., *Nature* **442**, 412–418 (2006).
- [3] Esfandeh, M., Mirabedini, S. M., Pazokifard, S., and Tari, M., *Colloids and Surfaces A* **302**, 11–16 (2007).
- [4] Grundke, G., Michel, S., Knispel, G., and Grundler, A. *Colloids and Surfaces A*, **1** **317**, 598–609 (2008).
- [5] Lee, D. Y., Oh, Y. I., Chung, K. H., Kim, K. M., and Kim, K. N., *J. Appl. Polym. Sci.* **92**, 2395–2401 (2004).
- [6] Gao, S. H., Gao, L. H., and Zhou, K. S., *Appl. Surf. Sci.* **257**(11), 4945–4450 (2011).
- [7] Parvinezadeh, M. and Ebrahimi, I., *Appl. Surf. Sci.* **257**, 4062–4068 (2011).
- [8] Conrads, H. and Schmidt, M., *Plasma Sources Sci. and Technol.* **9**, 441–454 (2000).
- [9] Fauchais, P., Vardelle, A., and Dussoubs, B., *J. Thermal Spray Technol* **10** (1), 44–66 (2004).
- [10] Murakami, T., Kuroda, S., and Osawa, Z., *J. Colloids and Interfaces* **202**, 37–44 (1998).
- [11] Ferguson, G. S., Chaudhury, M. K., Biebuyck, H., and Whitesides, G. M., *Macro molecules* **26**, 5870–5875 (1993).
- [12] Owen, M. J. and Smith, P. J., *J. Adh. Sci. Technol* **8**, 1063–1075 (1994).
- [13] Hillborg, H. and Gedde, U. W., *IEEE Dielectrics and Electrical Insulators* **6**, 703–717 (1999).
- [14] Tendero, C., Tixier, C., Pascal, T., Desmaison, J., and Leprince, P., *Spectrochimica Acta Part B: Atomic Spectroscopy* **61**, 2–30 (2006).
- [15] Encinas, N., Díaz-Benito, B., Abenojar, J., and Martínez, M. A., *Surf. Coat. Technol.* **205**, 396–402 (2010).
- [16] Owens, D. K. and Wendt, R. C., *J. Appl. Polym. Sci* **13**, 1741 (1969).
- [17] Van Oss, C. J., Good, R. J., and Chaudhury, M. K., *Langmuir* **4**, 884 (1986).
- [18] Bodas, D., Rauch, J. Y., and Khan-Mark, C., *European Polymer Journal* **44**, 2130–2139 (2008).
- [19] Zhu, Y., Otsubo, M., Honda, C., and Tanaka, S., *Polymer Degrad. and Stab.* **91**, 1448–1454 (2006).
- [20] Bhoj, A. N. and Kushner, M. J., *IEEE Transactions on Plasma Science* **33** (2), 250–251 (2005).